Bakker A., Fasano J.B., Leng D.E. (1994) Pinpoint Mixing Problems with Lasers and Simulation Software. Chemical Engineering, January 1994, page 94-100.

PINPOINT MIXING PROBLEMS

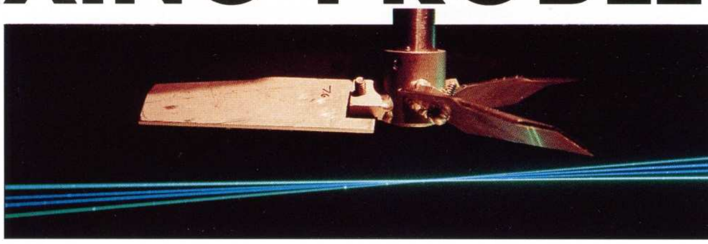

Dow Chemical Co.

WITH LASERS AND SIMULATION SOFTWARE

André Bakker and **Julian B. Fasano**,
Chemineer Inc.

Douglas E. Leng,
Dow Chemical Co.

One of the oldest unit operations in the chemical process industries (CPI), mixing has long been considered more of an art than a science. Although many rules of thumb and correlations of overall parameters have been developed to analyze and evaluate a mixing system, scaleup from a laboratory or pilot unit to a commercial plant is still risky. Processes that are sensitive to nonhomogeneities in a mixture pose special problems because the correlations do not take the local effects into account.

Increasingly, designers of various types of mixing equipment are turning to modern tools for flow analysis and visualization, such as computational fluid dynamics (CFD), laser Doppler velocimetry (LDV) and particle image velocimetry (PIV). Such quantitative design methods based on a fundamental understanding of the microscopic as well as macroscopic changes in the chemical and physical processes in the mixture are proving to be more effective than the traditional approaches.

Increased understanding of mixing is leading to more-reliable and optimized designs for stirred-tank reactors, for example. The sizes of these production vessels widely employed in the CPI can be quite small (30 L in pharmaceutical product development) or huge (two million liters in mining operations).

Because reactor design is often critical to the efficiency, operation and safety of a process, errors resulting from a lack of understanding of the mixing fundamentals can be costly. For example, the U.S. CPI are estimated to lose between \$1 and \$10 billion annually in productivity due to improper design of stirred reactors [*1*].

CFD, LDV and PIV permit in-depth analysis of the fluid mechanics and local mixing inside a stirred vessel. This leads to better process performance, lower failure rates, and eventually to increased productivity. Elaborated below are the basics of CFD, LDV and PIV, and the implications of their use in mixer design.*

A laser-Doppler velocimetry system (above) consists of a laser source, a mixing tank (not shown) and an impeller

Putting lasers to work

The first step to a better understanding of mixing lies in the accurate mapping of the flow field. Various experimental

*This article forms Part 1 of a series on the latest in mixing technology. Forthcoming articles will focus on the use of automated knowledge-based systems for optimizing mixer performance, and state-of-the-art design procedures for mixing equipment.

methods are used to analyze the flow field in mixing tanks.

These methods can be broken down into two general classes: One provides a "tunnel vision," while the other offers a "panoramic view." The first kind measures fluid properties and flow conditions at designated points in the flow field. Of course, an overall picture can be constructed via this method by successively measuring flow properties at various positions in the flow field. The second group of methods is used to measure the whole flow domain at once, giving a semi-instantaneous picture of the overall flow field.

There exist many measurement techniques for determining the fluid properties at a specified point. However, most of these depend on inserting such probes as hot wires, piezoelectric probes, vanes and pitot tubes that may disturb the local flow field. These methods will not be discussed in this article.

Today, the predominant nonintrusive method for point measurement of flow properties is LDV. Although expensive ($100,000–300,000), LDV is so well established that complete measurement systems (Figure 1) may be purchased off the shelf.

This system uses two laser beams: the measurement and the reference beams. When these two beams of light (albeit of small cross section) intersect at an angle of 2α, they create what is called the measurement volume at the "point" of intersection. Any tiny particle — either normally present in the fluid or deliberately added for flow visualization — passing through the measurement volume scatters the light illuminating the particle.

A typical particle size is 0.01–0.5 μm.

Modern flow-visualization techniques offer fresh insights

This is usually smaller than the smallest eddies or whirls that form in turbulent flows, which are of the order of 20 μm. The effect of the particles on the flow is therefore negligible. In fact, it is safe to assume that the trajectory of the particle represents fluid flow at a particular point.

Scattered light from the measurement beam and the unscattered light from the reference beam are mixed at a photodetector surface to give a "difference" signal. The velocity of the particle can be measured by analyzing this signal. Although this step involves complex signal analysis, the user need not be an expert in optical signal processing to get the most out of LDV. Often, all that is needed is adequate knowledge of how to operate the signal processors and interpret the output.

FIGURE 2. Streaklines around a disc-style impeller indicate fluid velocities at various points inside a vessel

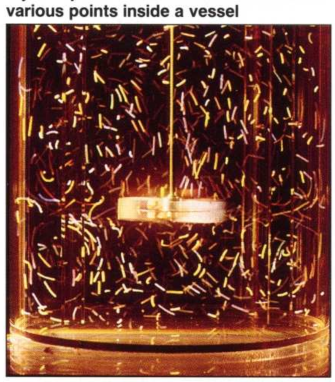

LDV measurements are made at a specific point in the tank over a period of time. Thus the measured velocities are time-averaged quantities. A picture of the entire flow field can be obtained by scanning the whole tank. Since these measurements cannot be made simultaneously at different locations, LDV is not suitable for studying time-dependent or unsteady-state flows.

When time-dependent flows must be measured, one needs to obtain a measurement of the whole flow field at a given instant in time. Among the various methods available for a snapshot of the flow field, perhaps the simplest is streamline photography.

In this method, translucent particles are added to a mixing tank that is illuminated by a flat beam of light, often called a "light sheet," which defines the measurement plane. The particles become visible only when they pass through, or are in the plane of, the light sheet. Streamlines can be created by taking pictures with an appropriate shutter speed (Figure 2). The particle streaks show the direction of fluid velocities at various points, with the length of the streaks being proportional to the fluid velocity at a given point. Pictures like this give a good *qualitative* description of the flow pattern.

When *quantitative* measurements of the flow patterns are required, one must resort to more-advanced methods, such as PIV [*2*]. Here also, one illuminates the mixing tank with a light sheet, usually from a laser source. By double-pulsing the light source, or by taking two successive pictures with a continuous light source, one obtains a double exposure of the particle field.

The velocity field is then calculated from the displacement of the particles during the exposure time. In the past,

FIGURE 1. The schematics show the configuration of a laser-Doppler velocimeter for mixing applications

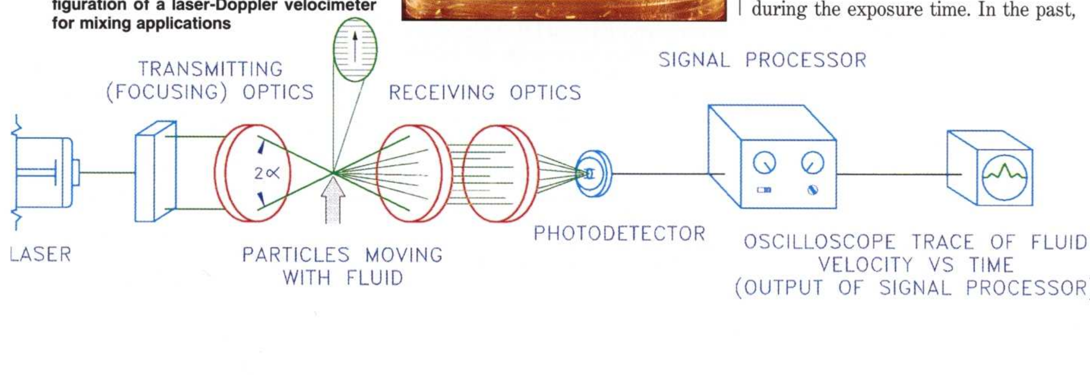

however, it was not always obvious which two images correspond to the same particle. Now there are analysis techniques available that use cross-correlation algorithms to identify and track the particles.

Among the methods discussed above for visualization of single-phase flows, LDV is the most popular due to the commercial availability of accurate and easy-to-use measurement systems. Although it requires nearly clear liquids and usually a transparent vessel made from glass or plastic, submersible optic probes are now available for use with metalwall vessels.

In a typical setup, the stirred tank is mounted stationary, and the LDV system is placed on a traversing mechanism. But the opposite arrangement is just as appropriate. Either arrangement makes it possible to obtain the whole flow field by incrementally moving either the tank or the laser source. Newer systems often use fiber-optic cables to connect the probes to the laser source. This makes movement of the optical paraphernalia much easier.

The advantage of LDV is that it allows very accurate measurements of

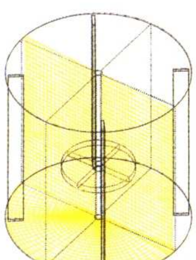

FIGURE 4. A stirred tank is divided into four sections, and each is subdivided into 25,000 grids or computational cells

both the mean velocity of the liquid at a point and the velocity fluctuations (around the mean) due to turbulence. Consequently, one of the main applications of LDV data is for the validation and testing of CFD models.

Visualizing gas-liquid flows

Flow of gas-liquid mixtures has been, and still is, notoriously difficult to analyze. As a result, most design procedures are based on correlations of overall quantities, such as power consumption, gas holdup and mass-

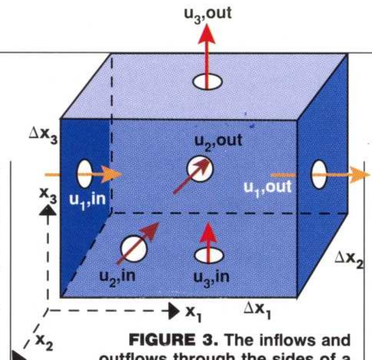

FIGURE 3. The inflows and outflows through the sides of a computational cell provide a convenient way to account for the conserved quantities, such as mass, energy and momentum

NOMENCLATURE

A	Chemical species
B	Chemical species
C_n	Concentration of chemical species *n*
F	External forces, N/m³
g	Acceleration due to gravity, m/s²
i	Index
j	Index (iCj)
k_i	Reaction rate constant
p	Pressure, Pa
R	Chemical species
S	Chemical species
u_i	Fluid velocity in x_i direction, m/s
x_i	Coordinates
X	Product yield distribution
μ	Fluid viscosity, Pa.s
ρ	Fluid density, kg/m³

transfer coefficient. Apart from the qualitative sketches obtained from flow-visualization studies, very little is known to date about the internal structure of gas-liquid dispersions. Especially at high gas-holdup conditions frequently encountered in the CPI, it is extremely difficult to see through a gas-liquid mixture. Even a laser beam is often completely scattered by the gas-liquid interfaces.

Only recently have devices become available to accurately measure local quantities in gas-liquid dispersions. Greaves and Barigou [3] use capillary suction probes to measure the bubble size in the outflow of a Rushton turbine. Fischer [4] uses an ultrasonic-Doppler technique to determine the velocities, gas-liquid interfacial areas and bubble-number densities in largescale fermenters. Their results give excellent insight into the gassed-flow pattern in stirred reactors.

Bakker [5] uses optical-fiber probes to measure local gas-holdup and bubble size in gassed-stirred reactors. His results have been used in the verification of a computer model for gas-liquid mixing in a stirred reactor.

These experimental techniques open new possibilities for the analysis of gassed stirred-tank reactors. For example, they can be used to map the patterns of gas-liquid dispersion, detect poorly mixed or aerated zones where microorganism starvation may occur. These tools can also provide data for the development and verification of new, advanced computer models for predicting gas-liquid flow behavior.

Equations of fluid mechanics

CFD is based on what are known as the conservation equations for mass, energy and momentum. The simplest of these is the equation for conservation of mass, also known as the continuity equation. The inflow and outflow of fluid streams are illustrated in a simple Cartesian coordinate system (Figure 3) for the sake of discussion here. (Using the more-natural cylindrical coordinate system for cylindrical stirred tanks makes the forms of the equations somewhat cumbersome, although one can switch back and forth using the available algorithms for coordinate transformation.) To ensure conservation of mass, the sum of the six streams must be 0:

$$\Delta x_2 \Delta x_3 (u_{1,out} - u_{1,in}) + \Delta x_1 \Delta x_3 (u_{2,out} - u_{2,in}) + \Delta x_1 \Delta x_2 (u_{3,out} - u_{3,in}) = 0 \quad \textbf{(1)}$$

This equation can be rewritten in differential form as:

$$\frac{\partial u_1}{\partial x_1} + \frac{\partial u_2}{\partial x_2} + \frac{\partial u_3}{\partial x_3} = 0 \quad \textbf{(2)}$$

A more compact way to write this equation is:

$$\frac{\partial u_i}{\partial x_i} = 0 \quad \textbf{(3)}$$

Here u_i stands for the velocity in direction x_i. The notation follows the so-called Einstein summation convention: Repetition of an index in the same term implies summation over all possible values of the index.

An equation for conservation of momentum can be derived in a similar fashion. This is more complicated because one has to incorporate viscous momentum transport and external forces, such as pressure and gravity. The equation for conservation of momentum in laminar flow reads:

$$\frac{\partial\left(\rho u_i u_j\right)}{\partial x_i} = \frac{\partial\left(\mu\left[\frac{\partial u_i}{\partial x_j}+\frac{\partial u_j}{\partial x_i}\right]\right)}{\partial x_i} - \frac{\partial p}{\partial x_j} + \rho g_j + F_j \qquad \mathbf{(4)}$$

The term on the left of the equal sign denotes the convective transport of momentum. The first term on the right represents the viscous transport of momentum, while the last three terms are the "production" terms, including pressure, gravity and external forces.

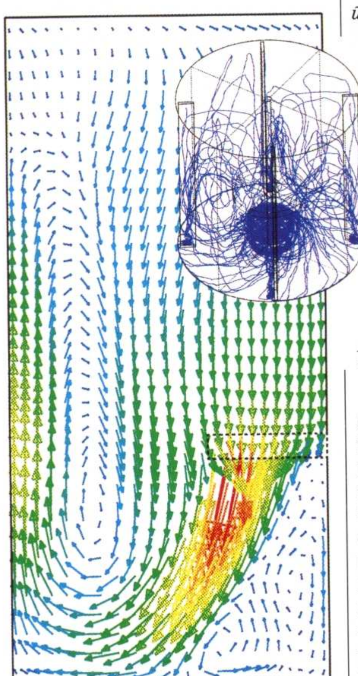

FIGURE 5. A pitched-blade turbine pumps down and generates a typical axial-flow pattern (one-half of the symmetrical flow field shown). Long, red arrows denote high velocities, while short, blue arrows denote relatively low velocities. The inset shows simulated random trajectories of solid particles. Note the stagnant or 'dead' zones behind the baffles and in the center at the tank bottom

Equations 3 and 4 are in fact four equations for four unknown quantities, namely pressure and the three velocity components. Thus, these equations form a "closed set," and are in principle solvable for the calculation of the flow field.

However, these equations hold only for laminar flow. The situation is much more complicated for turbulent flows, where fluid velocities exhibit random fluctuations. The fluid velocity at a certain point is now time-dependent, and is described by an average component u_i and a fluctuating component $u_i'(t)$:

$$\tilde{u}_i(t) = u_i + u_i'(t) \qquad \mathbf{(5)}$$

The fluctuating velocity component $u_i'(t)$ is a random function of time, which, by definition, is unknown for a given instant. The more-complicated momentum balance for the average flow now reads:

$$\frac{\partial\left(\rho u_i u_j\right)}{\partial x_i} = \frac{\partial\left(\mu\left[\frac{\partial u_i}{\partial x_j}+\frac{\partial u_j}{\partial x_i}\right]\right)}{\partial x_i} - \frac{\partial p}{\partial x_j} + \rho g_j + F_j + \frac{\partial\left(\rho \overline{u_i' u_j'}\right)}{\partial x_i} \qquad \mathbf{(6)}$$

The additional term in Equation 6 (compared to Equation 4) represents the correlation between the turbulent fluctuations in the three directions and is dependent on both the directional structure of the turbulence and on the magnitude of the velocity fluctuations. This term is commonly referred to as the Reynolds stress tensor. It creates an additional difficulty for modeling turbulent flows. Although analytical equations for the Reynolds stresses can be derived, the resulting set of equations is not a closed set due to the averaging process. This poses what is known as "a closure problem."

Various models for the Reynolds stress terms have been derived. Among the advanced turbulence models are the Algebraic Stress Model [*6*] and the newer Reynolds Stress Models [*7*].

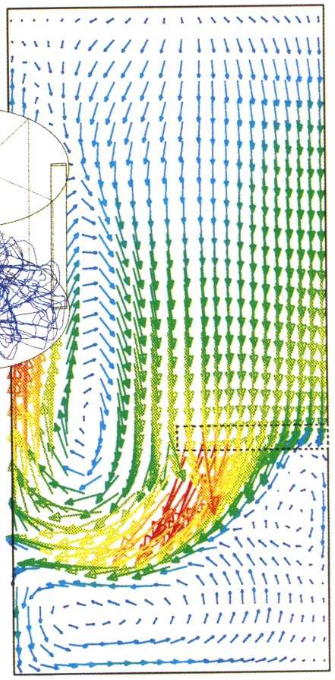

FIGURE 6. For the same tank as in Figure 5, a larger-diameter impeller pumps more radially, generating two flow loops under the shown half of the impeller. The flow at the tank bottom is weak and directed inward, inhibiting solids suspension (inset). The particles move around at the tank bottom, and are not suspended throughout the liquid bulk

How to apply CFD to mixing

Before beginning the flow calculations for a stirred tank, one must divide the tank geometry into small cells (Figure 4). This is commonly referred to as grid generation. The success of CFD-based simulation often depends on the creation of a suitable mesh or grid. Once the grid is set up, equations for the conservation of mass, heat and momentum, along with the quantities that account for the effects of turbulence and for species creation or removal by chemical reaction can then be solved by means of an off-the-shelf iterative numerical procedure.

An important part of the calculation is to satisfy the boundary conditions for the equations. As a rule, one sets the liquid velocity at the tank walls to be zero, which is known as the "no slip" boundary condition. Assuming that the liquid surface (or the liquid-air interface) is frictionless, one employs the so-called free-slip boundary condition at the given liquid level for the tank.

Proper specification of the input data (source terms) for the boundary conditions around the impeller is also important. There are many ways to model the forces and velocities induced by the impeller rotation. The most common is to use location-specific, time-averaged velocities in the impeller discharge region. In actuality, however, the fluid velocities are time dependent, and time-averaging is not strictly meaningful because when the impeller blades pass a given point, they create periodic surges in flow and pressure.

A full description of flows around the blades is theoretically possible, but extremely demanding in terms of computer time needed to do the computations. Newer techniques that can be better adapted to describing the unsteady conditions around the impeller are also being tried out. One such technique allows the user to rotate the vessel walls while keeping the impeller stationary, and another uses a rotating mesh [*8*, *9*].

Because of the added complexity of the newer methods, engineers find it more convenient to use available experimental data on impeller-induced flows for a wide range of impeller sizes and geometries. In this case, the experimental data are used as input for the CFD model.

Experienced CFD users look for symmetry in the stirred vessel being simulated. When the vessel is equipped with standard baffles, it is often adequate to simulate only a quarter of the vessel. Also, for a baffled vessel with predominantly axial and radial flow, it can sometimes be assumed that the flow field is symmetrical around the shaft. The flow properties are then independent of the tangential coordinate, leading to a so-called two-dimensional model. Simplifications like these often greatly cut down on computing time.

For example, in simulating the flow patterns generated by a 45-deg-pitched-blade turbine, experimental discharge data serve as the impeller source terms. This impeller pumps downwards, and creates one large flow loop (Figure 5).

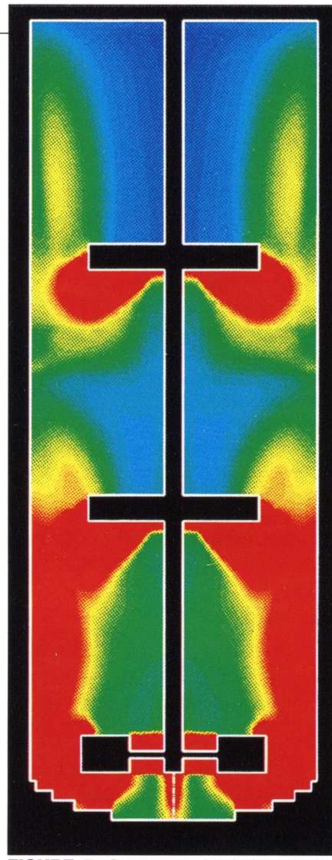

FIGURE 7. Computer simulation shows the mass-transfer-rate distribution in a fermentor. Red and blue regions denote areas with high and low values of the mass-transfer rates, respectively

When the flow pattern is known, one can use it to visualize the suspension of solid particles (Figure 5; inset). The lines show the semi-random trajectories of solid particles in the tank. In this case, the tank is well mixed, albeit not uniform in solids concentration. But the particles appear to be well suspended.

When the diameter of the impeller is increased (from 0.4 to 0.5 m), and its speed is decreased so that the power consumption remains constant, the flow pattern undergoes appreciable changes (Figure 6). The jet coming from the impeller no longer reaches the vessel bottom, instead it bends off toward the vessel wall. A large circulation loop with inward-directed velocities is formed at the tank bottom. In this case, the solid particles are very poorly suspended (Figure 6; inset).

The particles appear to be concentrated in the flow loop at the bottom of the tank. This behavior has been verified by experimental data. Conventional design procedures for solids suspension are based on overall power consumption, and do not anticipate these differences in performance due to impeller and tank geometry. An engineer unaware of the importance of these effects of geometry, which are apparent to CFD users, is likely to make a serious design error.

In certain cases, CFD can be used to predict the flow patterns for gas-liquid mixtures. These models are fairly new, however, and are not yet included in commercially available CFD codes. One code, called Ghost! (Gas Holdup Simulation Tool!), developed at Delft University in the Netherlands has been successfully used to generate a color-coded map of the local mass-transfer rate in a stirred tank (Figure 7).

Mass transfer rates are high in the impeller discharge region, where the mixture is vigorously agitated and the flow is highly turbulent. Also note that farther from the impeller, mass-transfer rates are much lower. Results like these, which provide excellent qualitative and quantitative information, are next to impossible to obtain experimentally. Clearly, the real value of CFD tools, such as Ghost!, comes in the prediction of the performance of gas-liquid systems in scaled-up chemical reactors and fermenters.

Off-the-shelf software

The number of commercially available CFD codes has been growing steadily. A comprehensive overview of commercial codes is available elsewhere [*10*]. The codes often used to analyze stirred tanks include Fluent, Phoenics, Fidap, Star-CD, and Harwell Flow-3D.

A few companies have developed their own specialized codes. Most of the results presented in this article are based on calculations performed with Fluent V3. Today, most commercial codes offer a wide variety of numerical algorithms, physical models, and grid-generation options. When purchasing a commercial CFD package for mixing applications, a buyer should be sure to look for the following features:

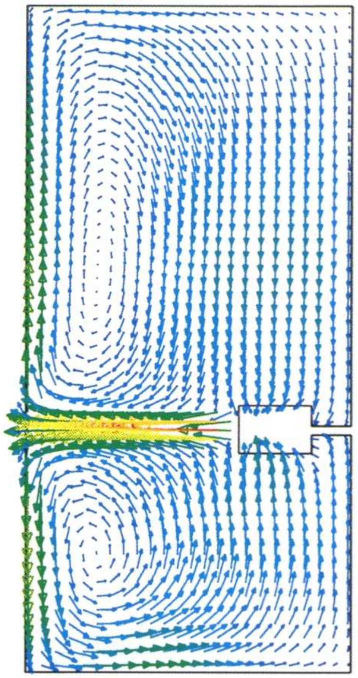

FIGURE 8. The arrows show the typical flow pattern in a tank equipped with a radial 'pumping' turbine

- Ability to use higher-order numerical differencing schemes, such as power law and quadratic upwind interpolation for convection kinematics (Quick)
- Incorporation of nonisotropic turbulence models, such as the Algebraic Stress Model [*6*] and the newer Reynolds Stress Models [*7*]
- Flexibility in the grid generation process: For top-entering impellers in a cylindrical tank, one can use a simple cylindrical coordinate system; for more complex geometries, such as side-entering impellers and tanks with curved bottoms, one should use a so-called body fitted coordinate (BFC) system
- Vectorizability or configurability of the code for use on supercomputers or massively parallel machines

CFD has long been accessible only to fluid dynamicists and theoreticians, but the newer commercial codes make CFD attractive to nonexperts. It should be kept in mind, however, that the user interface is an important factor in the usability of a code. Most CFD vendors are offering trial periods for their products, and provide sufficient training on how to get started.

Apart from the software, the hardware should be given some thought, too. During calculation of the flow patterns in a typical stirred tank, one may have to deal with around 25,000 grid nodes and solve the resulting hundreds of thousands of equations.

Computation of the results based on a nonisotropic turbulence model typically takes about six hours on a 25-Mflops (million floating-point operations per second) Unix workstation, and requires 32 Mbyte of random access memory. When using a 80486-based personal computer with sufficient memory, the calculation time will be one to two orders of magnitude greater, resulting in a calculation time of several days to a week. On the other hand, when a supercomputer, such as a CRAY-YMP C90, is used, the calculation time is less than an hour, allowing fast evaluation of alternative configurations for mixing equipment. The hardware choice depends on the available budget, and the number and size of problems expected to be analyzed.

CFD on mixing with reaction

An excellent example of the application of CFD to the design of turbine-stirred reactors is in the calculation of the reaction yield [*11*]. In this study, one tank has a volume of 0.03 m^3, while the others are substantially larger (0.6 m^3 and 0.9 m^3). The CFD results are verified experimentally and used to evaluate scaleup rules.

A typical flow pattern in such a reactor is shown in Figure 8. Figure 9 shows a comparison between axial velocities as measured with LDV and as predicted by CFD for such a tank [*5*]. Clearly, the predicted and measured velocities compare well, giving confidence in the CFD model.

As a simple case study, one can investigate the following competitive-consecutive reaction system [*12*]:

$$A + B \xrightarrow{k_1} R$$

$$B + R \xrightarrow[k_1 \gg k_2]{k_2} S$$

The experiments and simulations start with the tanks filled with an aqueous solution of reactant A. Reactant B is added near the top of the tank. The concentrations of the reactants are monitored until a steady state is reached. The yield distribution of undesirable product, S, is expressed as:

$$X = \frac{2C_S}{C_R + 2C_S} \quad \textbf{(7)}$$

Researchers have found that the experimental data and the results of the computer model compare well on both scales of 30- and 600-L reactors (Figure 10). This comparable agreement shows how well CFD models can be used to predict flow-sensitive reaction yields at all scales.

The experimental data are also used to evaluate some commonly used scaleup criteria. Figure 11 shows the gross

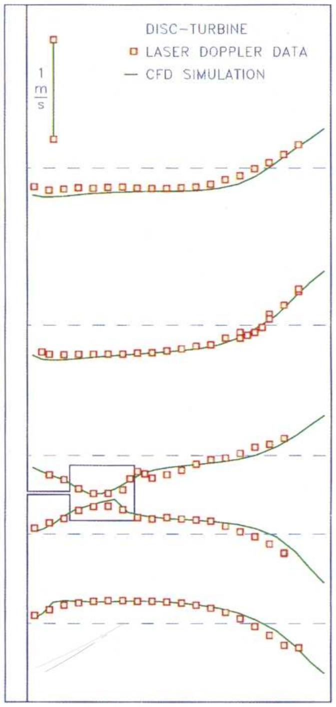

FIGURE 9. The axial flow velocities measured with LDV (data points indicated by squares) and predicted by CFD software (solid lines) show good agreement throughout a 0.3-m-dia. tank. The distance from the dotted baseline corresponds to the axial velocity in that region

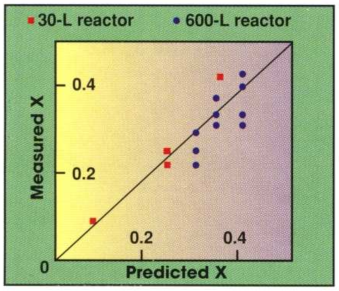

FIGURE 10. Directly measured values of product yield distribution agree well with those obtained from CFD simulation, for both 30- and 600-L reactors

discrepancies in the product yield distribution X for the two reactor sizes (of 30 and 900 L) as a function of impeller tip speed, power per unit volume and mixing time. None of these commonly used scaleup rules are capable of correlating the reaction yield at the two reactor scales. Thus, performing experiments at a small scale and using one of these traditional scale up rules may lead to an incorrect prediction of the reaction yield at the larger scale.

On the other hand, the CFD simulations predict the reaction yield within $\pm10\,\%$ at both scales. This clearly demonstrates the power of CFD over traditional rules of thumb when scaling up chemical reactors.

Peering into the future of CFD

The flow analysis and visualization tools are expected to have a major impact on the way process equipment is designed in the future. The examples illustrate how CFD can be used to provide detailed design information where traditional scaleup correlations and design rules are deficient. This is important especially for the scaleup of chemical reactors in the CPI.

A major advantage of CFD is that the models are scale-independent and, once verified, they can be used to simulate the behavior of any larger reactor. However, blind application of the codes on the belief of absolute accuracy should be avoided at all costs.

Further, it must be remembered that the CFD models are nothing more than convenient mathematical representations of what actually goes on in a mixer. They should not be oversold by claims of infallibility, especially in circumstances when the underlying assumptions of the models break down.

It is expected, however, that the rapid development of CFD codes, powerful workstations and the availability of more and better experimental data will soon lead to technologies that can be used by those who are not necessarily experts in computational fluid dynamics or complex reaction kinetics .

Eventually, these developments in modeling mixing action should lead to design of safer reactors and improved process efficiency. They could also result in better utilization of idle mixing equipment via its more-rapid deployment in a wide variety of process applications throughout a plant. ■

Edited by Gulam Samdani

Acknowledgement

The authors wish to thank John C. Middleton from ICI Chemicals and Polymers Ltd. for his permission to use the data presented in Figures 10 and 11.

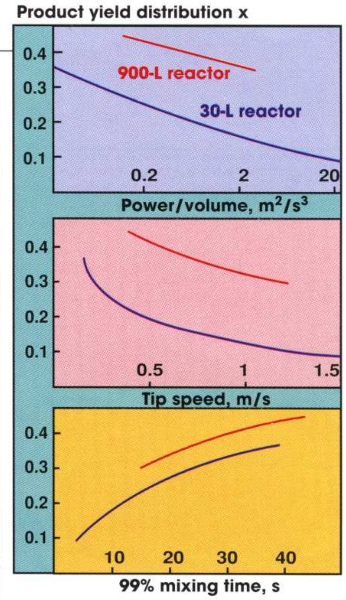

FIGURE 11. The measured values of product yield distribution depend on the reactor sizes. None of the often-used scaleup criteria can correlate the data at such different scale. Having no such limitations, CFD software provides a superior alternative to the scaleup criteria

References

1. "Mixing 3A Workshop: Industrial Mixing Needs," University of Maryland, March 22–23, 1989.
2. Bjorkquist, D. C., Particle Image Velocimetry for Determining Structures of Turbulent Flow Lines, TSI Inc. (Bridgeville, Pa.), Vol. 6 (1), pp. 3–8, 1991.
3. Greaves, M., and Barigou, M., The Internal Structure of Gas-Liquid Dispersions in a Stirred Reactor, *Proc. 6th Eur. Conf. on Mixing*, Pavia, Italy, pp. 313–320, 1988.
4. Fischer, J., and others, Structure of the Gas-Phase Motion in Aerated Stirred Tank Reactors, *AIChE Symposium Series* 286, Vol. 88, pp. 98–102, 1991.
5. Bakker, A., Hydrodynamics of Stirred Gas-Liquid Dispersions, PhD Thesis, Delft University of Technology, Delft, the Netherlands, 1992.
6. Rodi, W., Turbulence Models and Their Application in Hydraulics — A State of the Art Review, Int. Assn. for Hydraulic Research, Delft, the Netherlands, 1980.
7. Users' Manuals on Fluent V4, Fluent Inc., Lebanon, N.H.
8. Perng C. Y., and Murthy J. Y., A Moving Mesh Technique for the Simulation of Flow in Mixing Tanks, AIChE Annual Meeting, Miami Beach, paper 109b, Nov. 1992.
9. Gosman, A. D., and others, Full Flow Field Computation of Mixing in Baffled Stirred Vessels, AIChE Annual Meeting, Miami Beach, paper 109c, Nov. 1992.
10. "How To CFD," Silicon Graphics Computer Systems, Mountain View, Calif., 1992.
11. Middleton, J. C., and others, Computations of Flow Fields and Complex Reaction Yield in Turbulent Stirred Reactors and Comparison with Experimental Data, *Chem. Eng. Res. Des.*, Vol. 64, pp. 18–22, Jan. 1986.
12. Bourne, J. R., and others, Mixing and Fast Chemical Reaction I — Test Reactions to Determine Segregation, *Chem.Eng.Sci.*, Vol. 36 (10) p. 1643, 1981.

The authors

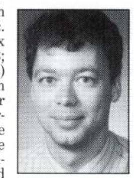

André Bakker is a research engineer at Chemineer Inc. (5870 Poe Avenue, P.O. Box 1123, Dayton, OH 45401-1123; tel: (513) 454-3200; fax: (513) 454-3379). He has been with the company since 1991 after completing his doctoral dissertation on gas-liquid mixing. He holds an engineering degree from Delft University of Technology, the Netherlands, and his Ph.D. is in applied physics. His specialization includes computational fluid dynamics in mixing processes.

Julian B. Fasano is technical director at Chemineer. He has been with the company for 22 years, and is responsible for research and development, and custom equipment design. He holds a B.Sc. in chemical engineering and an MBA from the University of Dayton, and an M.Sc. in chemical engineering from Lehigh University. Currently, he is pursuing his doctorate in materials engineering at the University of Dayton.

Douglas E. Leng is a senior research scientist in the Central Research & Development Engineering Research & Process Development Laboratory of The Dow Chemical Co. (Midland, Mich.). During the last 27 years (out of his 37 years at Dow), he has been involved in mixing and multiphase research, applications, problem-solving, and engineering administration. He obtained a B.Sc. and an M.Sc. from Queen's University (Kingston, Ont.), and a Ph.D. from Purdue University. A fellow of the American Institute of Chemical Engineers and a member of the American Chemical Soc., he was chairman of the Engineering Foundation Conference on Mixing in 1981.